Investigation on Electromagnetic Scattering form Dielectric Soil Rough Surface with a PEC Object Embedded in It

Hongmei Miao[1] **and Pengju Yang**[2]

[1]College of Physics and Electronic Information, Yanan University, Yan'an 71600, China
[2]School of Physics and Optoelectronic Engineering, Xidian University, Xi'an 710071, China

Abstract— In this paper, electromagnetic (EM) scattering from one-dimensional dielectric soil rough surface with a perfect electric conductor (PEC) embedded in it is investigated by method of moments (MoM) for HH polarization. The soil rough surfaces are modeled as realizations of a Gaussian random process with the exponential spectrum, while the tapered incident wave is chosen to reduce the truncation error. Several numerical results are presented to investigate the impact of rough surface parameters of rms height and correlation length on the bistatic scattering coefficient (BSC), while the influence of the size and position of the object on the BSC is discussed.

1. INTRODUCTION

Over the past several decades, a significant amount of research efforts has been spent toward developing viable buried object detection techniques, which is of great value in the detection of buried landmines, pipes and other buried objects of interest. The problem of detecting and imaging underground objects with electromagnetic sensors relies on accurate computational modeling which is challenging because of the complexity of the realistic ground surface. There are many difficulties associated with detecting objects beneath the ground due to the existence of clutter and low electromagnetic wave penetration into moist soil. The analytical algorithm has been applied to solve the problem of EM scattering from 2-D dielectric circular cylinder under beneath a slightly rough surface [1]. Although the analytical method is the computational simplicity and high efficiency, the disadvantage of the analytical method limited its applicability to canonical geometries, and to a small roughness rough surface. Consequently, one has to resort to numerical methods to deal with electromagnetic scattering from targets located below a dielectric rough surface [2–4].

Consequently, this paper is devoted to an investigation of EM scattering from soil rough surface with a perfect electric conductor (PEC) embedded in it.

2. THEORETICAL MODEL

2.1. Soil Surface Model

A rough surface is sampled at N points with spacing Δx over a simulated length $L = (N-1)\Delta X$. The altitude of each point $x_m = (m-1)\Delta x$ $(m = 1, \ldots, N)$ can be generated by (1)

$$f(x_m) = \frac{1}{L} \sum_{n=-N/2+1}^{N/2} F(k_n) \exp(ik_n x_m) \tag{1}$$

For $n \geq 0$

$$F(k_n) = \sqrt{2\pi L W(k_n)} \cdot \begin{cases} [N(0,1) + iN(0,1)]/\sqrt{2} & n \neq 0, \quad N/2 \\ N(0,1) & n = 0, \quad N/2 \end{cases} \tag{2}$$

For $n < 0$, $F(k_n) = F^*(k_{-n})$, where the asterisk represents a complex conjugate. $N(0,1)$ is a random variant with a Gaussian distribution of zero mean and unit variance. $k_n = \frac{2\pi n}{L}$.

Because land surfaces, including soil surfaces, have large slopes and fine-scale features and the exponential correlation surfaces have fine-scale features as depicted in Figure 1(b), it is reasonable to adopt exponential correlation spectrum in modeling randomly rough surface [6]. Furthermore, extensive soil rough surface profiles have been measured and the correlation functions were extracted from such profiles. It was concluded that the correlation functions were close to exponential correlation functions. Meanwhile, the results from exponential correlation functions are in much better agreement with radar measurements [6]. In this paper, randomly rough surfaces are modeled as realizations of a Gaussian random process with the exponential spectrum, and it can easily be generated by employing the spectrum method which has been widely used in the calculation of wave scattering.

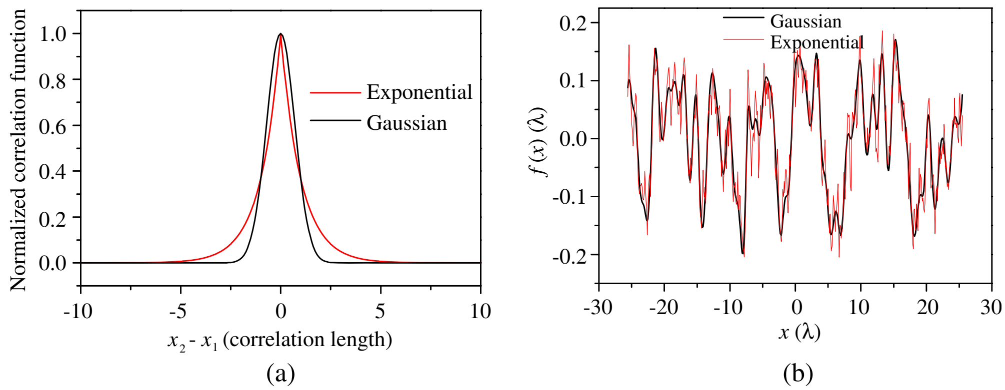

Figure 1: Comparison between surfaces with the Gaussian correlation function and exponential correlation function. (a) Normalized autocorrelation function; (b) 1-D rough surface profiles.

2.2. Composite Scattering Model

The basic geometry considered in this paper is that a PEC object is located below the dielectric rough surface with rms heights h and correlation length l. The height profile functions satisfy $\langle f_1(x)\rangle = 0$. The space is separated into two regions filled with different media by the rough interface: the upper medium denoted by $\Omega_0(\mu_0, \varepsilon_0)$ assumed to be free space, and the lower media represented by $\Omega_1(\mu_1, \varepsilon_1)$. The media involved in this study is supposed to be nonmagnetic, that is, $\mu_1 = \mu_0$. The time dependence of $\exp(-i\omega t)$ is assumed and omitted throughout this paper, where i denotes unit imaginary number. $\bar{k}_i$ and $\bar{k}_s$ are the incident and scattering wave vector, respectively. θ_i and θ_s are the incident and scattering angle, respectively. H represents the height of the object. Let ψ_0 and ψ_1 denote the fields in region 0 and region 1, respectively. Let $\bar{r}' = x'\hat{x} + z'\hat{z}$ and $\bar{r} = x\hat{x} + z\hat{z}$ represent source and field points, respectively.

Applying the Green's theorem to Ω_0, and Ω_1, respectively, one can obtain the surface integral equations for calculating EM scattering from the one-dimensional soil rough surfaces with a PEC object embedded in the lower media.

$$\frac{1}{2}\psi_0(\bar{r}) - PV\int_{S_r} ds'\hat{n}'\cdot\left[\psi_0(\bar{r}')\nabla' G_0(\bar{r},\bar{r}') - G_0(\bar{r},\bar{r}')\nabla'\psi_0(\bar{r}')\right] = \psi_{inc}(\bar{r}) \quad \bar{r}\in S_r \tag{3}$$

$$\begin{aligned}&\frac{1}{2}\psi_1(\bar{r}) + PV\int_{S_r} ds'\hat{n}'\cdot\left[\psi_1(\bar{r}')\nabla' G_1(\bar{r},\bar{r}') - G_1(\bar{r},\bar{r}')\nabla'\psi_1(\bar{r}')\right]\\ &-\int_{S_o} ds'\hat{n}'\cdot\left[\psi_1(\bar{r}')\nabla' G_1(\bar{r},\bar{r}') - G_1(\bar{r},\bar{r}')\nabla'\psi_1(\bar{r}')\right] = 0 \quad \bar{r}\in S_r\end{aligned} \tag{4}$$

$$\begin{aligned}&\frac{1}{2}\psi_1(\bar{r}) + \int_{S_r} ds'\hat{n}'\cdot\left[\psi_1(\bar{r}')\nabla' G_1(\bar{r},\bar{r}') - G_1(\bar{r},\bar{r}')\nabla'\psi_1(\bar{r}')\right]\\ &-PV\int_{S_o} ds'\hat{n}'\cdot\left[\psi_1(\bar{r}')\nabla' G_1(\bar{r},\bar{r}') - G_1(\bar{r},\bar{r}')\nabla'\psi_1(\bar{r}')\right] = 0 \quad \bar{r}\in S_0\end{aligned} \tag{5}$$

Note that in (3)–(5), the PV refers to the Cauchy principal value integral and $G_0(\bar{r},\bar{r}') = (i/4)H_0^{(1)}$ $(k_0|\bar{r}-\bar{r}'|)$, $G_1(\bar{r},\bar{r}') = (i/4)H_0^{(1)}(k_1|\bar{r}-\bar{r}'|)$ are the Green's function in region Ω_0 and Ω_1, respectively. $H_0^1(\cdot)$ is the zeroth-order Hankel function of the first kind. It should be pointed that the surface integral Equations (3)–(5), are applied to both TE and TM polarizations. The only differences between them is the integral term corresponding to object in surface integral Equation (5), and the surface integral (5) can readily be reduced to TE or TM case in terms of the boundary conditions.

In this paper, to avoid artificial edge diffraction resulting from the finite length of the simulated rough surface, the following Thorsos's tapered plane wave [7] rather than the generally used plane wave is chosen as the incident field.

$$\psi_{inc}(\bar{r}) = \exp\left[ik_0(x\sin\theta_i - z\cos\theta_i)(1+w(\bar{r}))\right]\cdot\exp\left(-(x+z\tan\theta_i)^2/g^2\right) \tag{6}$$

where g is the tapering parameter controlling the tapering length of the incident wave. The additional factor in the phase term of the Thorsos's tapered plane wave is $w(\bar{r}) = [2(x+z\tan\theta_i)^2/g^2 - 1]/(k_0 g\cos\theta_i)^2$.

One applies the MoM with point matching and pulse basis functions. From boundary conditions of continuity of tangential electric and magnetic field the set of integral Equations (3)–(5), one obtain linear system corresponding to the scattering problem.

Upon solving the matrix equation by utilizing MoM algorithm, the surface fields and their normal derivatives can be obtained. When the point $\bar{r}$ is located in the far field, the scattered field $\psi_s(\bar{r})$ in space Ω_0 is (7)

$$\psi_s(\bar{r}) = \frac{i}{4}\sqrt{\frac{2}{\pi k_0 r}}\exp\left(-i\frac{\pi}{4}\right)\exp\left(ik_0 r\right)\psi_s^{(N)}(\theta_s) \tag{7}$$

where

$$\psi_s^N(\theta_s) = \int_S ds\left[\psi(\bar{r})\left(-i\hat{n}\cdot\bar{k}_s\right) - \hat{n}\cdot\psi(\bar{r})\right]\exp\left(-i\bar{k}_s\cdot\bar{r}\right) \tag{8}$$

The normalized far-field bistatic scattering coefficient (BSC) with the Thorsos tapered plane wave incidence is defined as (9)

$$\sigma(\theta_s) = \frac{\left|\psi_s^N(\theta_s,\theta_i)\right|^2}{g\sqrt{\frac{\pi}{2}}\cos\theta_i\left(1-\frac{1+2\tan^2\theta_i}{2k_0^2g^2\cos^2\theta_i}\right)} \tag{9}$$

3. NUMERICAL RESULTS AND DISCUSSION

In this paper, the numerical simulations are conducted at a frequency $f = 1.2$ GHz. At $f = 1.2$ GHz, the relative permittivity of soil rough surface is taken as $\varepsilon_r = 9.77+0.48i$. Unless specified otherwise, the parameters of the rough surfaces are taken as $h = 0.1\lambda$, $l = 1.0\lambda$, respectively. The length of the soil rough surface is $L = 51.2\lambda$ with sampling step $\Delta x = \lambda/10$. Unless specified otherwise, the radius of the cylinder is $r = 1.0\lambda$. The results are presented here over 50 Monte Carlo realizations of rough surface for HH polarization.

Figure 2 presents the bistatic scattering coefficient (BSC) versus the scattering angle with different rough surface parameters of rms height and correlation length, respectively. One can observe that there exists an obvious peak in the specular direction for smaller rms height, which is attributed to the fact that a smaller rms height leads to a smaller roughness of the rough surface, giving rise to an obvious peak in the specular direction. The backscattering enhancement is also observed with rms height increasing, which is due to the fact that the roughness of the rough surface increases with rms height increasing. The influence of correlation length is also investigated in Figure 2. One can readily find backscattering enhancement with correlation length decreasing, which is attributed to the fact that roughness of the rough surface increases with correlation length decrasing.

In Figure 3, the dependency of the BSC on the size and the location of the cylinder are investigated. One can observe that, with the radius of the cylinder increasing, the BSC increases at non-specular region. It is readily found that the BSC almost unchanged in the specular direction, which is attributed to the fact that the total scattering strength depends mainly on the soil rough surface rather than the object due to the fact that the size of the object is really small compared to the soil rough surface. One can also observe that, the impact of the height of the cylinder is small with the height of the cylinder increasing due to the absorption of the lossy dielectric surface.

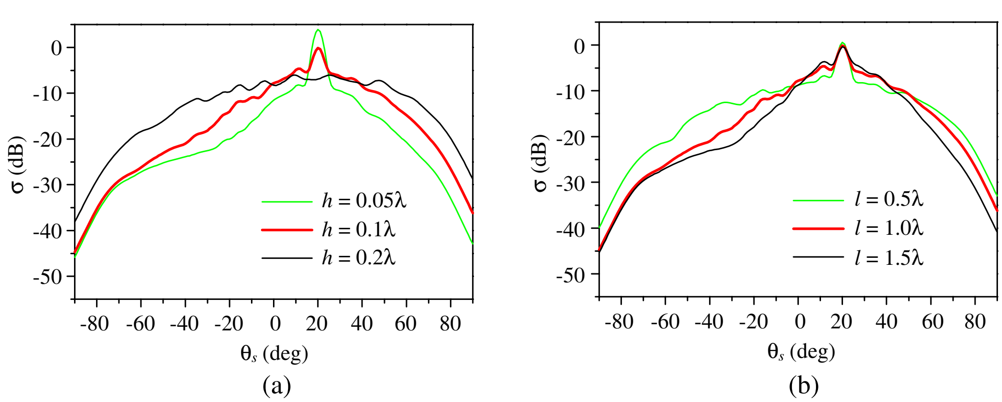

Figure 2: BSC versus the scattering angle with different rough surface parameters.

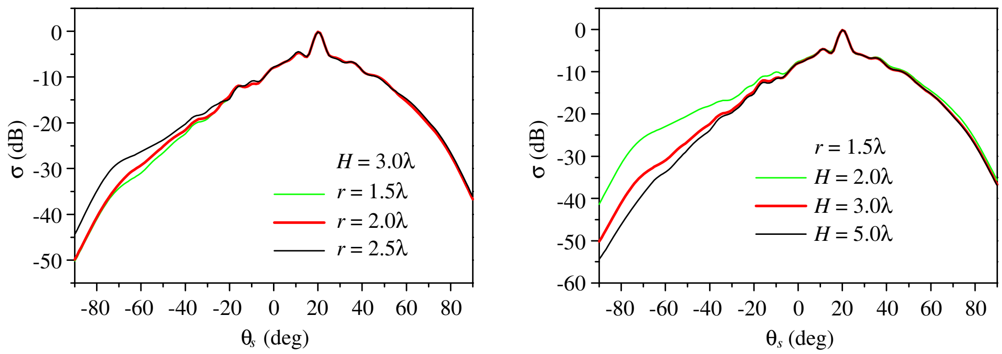

(a) (b)

Figure 3: BSC versus the scattering angle with different object parameters.

4. CONCLUSION

In this paper, the influence of the rough surface parameters and the parameters of the size and the positon of the cylinder on bistatic scattering coefficient is investigated by utilizing MoM. Numerical results have showed that the rms height and correlation length of the rough surface have significant influence on the angular distribution the BSC while the impact of the size and the position of the cylinder is relatively small under certain condition considered in this paper due to the fact that total scattering strength depends mainly on the soil rough surface rather than the object.

ACKNOWLEDGMENT

The authors would like to thank the anonymous reviewers for their helpful and constructive suggestions and Investigstion on Electromagnetic Scattering from the Land Surface and the Land Parametic Inversion of Northern Shanxi Region, National Natural Science Foundation of China (Grant No. 61379026).

REFERENCES

1. Lawrence, D. E. and K. Sarabandi, "Electromagnetic scattering from a dielectric cylinder buried beneath a slightly rough surface," *IEEE Trans. Antennas Propag.*, Vol. 50, 1368–1376, 2002.
2. Wang, X., C.-F. Wang, Y.-B. Gan, and L.-W. Li, "Electromagnetic scattering from a circular target above or below rough surface," *Progress In Electromagnetics Research*, Vol. 40, 207–227, 2003.
3. Zhang, G. F., L. Tsang, and Y. Kuga, "Studies of the angular correlation function of scattering by random rough surfaces with and without a buried object," *IEEE Trans. Geosci. Remote Sensing*, Vol. 35, 444–453, 1997.
4. Bourlier, C., G. Kubické, and N. Déchamps, "Fast method to compute scattering by a buried object under a randomly rough surface: PILE combined with FB-SA," *J. Opt. Soc. Am. A*, Vol. 25, 891–902, 2008.
5. Tsang, L., J. A. Kong, K. H. Ding, and C. O. Ao, *Scattering of Electromagnetic Waves: Numerical Simulations*, Vol. 2, Wiley-Interscience, New York, 2001.
6. Tsang, L., K. H. Ding, S. W. Huang, and X. L. Xu, "Electromagnetic computation in scattering of electromagnetic waves by random rough surface and dense media in microwave remote sensing of land surfaces," *Proc. IEEE*, Vol. 101, 255–279, 2013.
7. Thorsos, E. I., "The validity of the Kirchhoff approximation for rough surface scattering using a Gaussian roughness spectrum," *J. Acoust. Soc. Am.*, Vol. 83, 78–92, 1988.